Technology in Cancer Research & Treatment
2017, Vol. 16(6) 749–757

DOI: 10.1177/1533034616681670
journals.sagepub.com/home/tct
SAGE

Proton Grid Therapy: A Proof-of-Concept Study

Thomas Henry, MSc[1], Ana Ureba, PhD[1], Alexander Valdman, MD, PhD[2], and Albert Siegbahn, PhD[1]

Abstract

In this work, we studied the possibility of merging proton therapy with grid therapy. We hypothesized that patients with larger targets containing solid tumor growth could benefit from being treated with this method, proton grid therapy. We performed treatment planning for 2 patients with abdominal cancer with the suggested proton grid therapy technique. The proton beam arrays were cross-fired over the target volume. Circular or rectangular beam element shapes (building up the beam grids) were evaluated in the planning. An optimization was performed to calculate the fluence from each beam grid element. The optimization objectives were set to create a homogeneous dose inside the target volume with the constraint of maintaining the grid structure of the dose distribution in the surrounding tissue. The proton beam elements constituting the grid remained narrow and parallel down to large depths in the tissue. The calculation results showed that it is possible to produce target doses ranging between 100% and 130% of the prescribed dose by cross-firing beam grids, incident from 4 directions. A sensitivity test showed that a small rotation or translation of one of the used grids, due to setup errors, had only a limited influence on the dose distribution produced in the target, if 4 beam arrays were used for the irradiation. Proton grid therapy is technically feasible at proton therapy centers equipped with spot scanning systems using existing tools. By cross-firing the proton beam grids, a low tissue dose in between the paths of the elemental beams can be maintained down to the vicinity of a deep-seated target. With proton grid therapy, it is possible to produce a dose distribution inside the target volume of similar uniformity as can be created with current clinical methods.

Keywords

proton therapy, grid therapy, proton grid therapy, spatially fractionated beams, treatment planning, new treatment method

Abbreviations

CI, conformity index; CT, computed tomography; 1-D, 1-dimensional; 2-D, 2-dimensional; IMPT, intensity-modulated proton therapy; PGT, proton grid therapy; PTV, planning target volume; PVDR, peak-to-valley dose ratio; SBRT, stereotactic body radiation therapy

Received: August 05, 2016; Revised: October 04, 2016; Accepted: October 28, 2016.

Introduction

For over a century, grid therapy has been carried out on a small scale at a few clinics around the world with the aim of reducing the size of large bulky tumors.[1,2] Historically, unidirectional (occasionally parallel opposing) photon beam grids have been used for grid therapy. The elemental beams, building up the grid, typically have had sizes of approximately 1 cm or larger at the patient surface and have been separated with a similar distance. The beam grid array has been used to irradiate the patients with a chessboard-shaped irradiation pattern. At the

[1] Medical Radiation Physics, Department of Physics, Stockholm University, Stockholm, Sweden
[2] Department of Oncology and Pathology, Karolinska University Hospital, Stockholm, Sweden

Corresponding Author:
Thomas Henry, MSc, Medicinsk Strålningsfysik Box 260, Stockholms Universitet, 171 76 Stockholm, Sweden.
Email: thomas.henry@fysik.su.se

onset of grid therapy, the aim was to reduce the skin toxicity observed in the early days of radiotherapy.[3] Later, it was realized that not only the skin would benefit from leaving volumes of unirradiated cells in between the radiation beams but that the toxicity is also reduced for other organs located deep beneath the skin.[4] The dose delivered to the target in grid therapy has typically alternated between very high peak and lower valley doses.

In recent years, a large number of patients have been treated for bulky head and neck, thoracic, and abdominal cancers using the grid technique, with impressive results.[5-10] Typically, a large dose, for example, 15 Gy (inside each of the small beams building up the grid), has been given to the targeted disease in a single fraction. Sometimes, it has been combined with other therapies. Grid therapy has been found to produce limited toxicity in the surrounding sensitive tissues, considering the high in-beam doses given. Although certain subvolumes of the target (in between the beams) are given lower doses, significant reductions in the sizes of large tumors have been demonstrated.

The high normal tissue tolerance to beam grids is closely related to the so-called dose–volume effect, which has been described for single beams.[11] Experiments with beam sizes in the millimeter to centimeter range with both protons and photons have demonstrated that the tolerance doses for certain biological endpoints are rising with reduced beam sizes.[11,12] The migration of cells from unirradiated to irradiated volumes and an improved vascular repair if only a short segment of a vessel is irradiated have been stated as reasons for the improved tissue repair for smaller beam sizes. Experiments and preclinical radiotherapy trials with photon and ion beam grids, containing beam elements of widths in the micrometer to millimeter range, have more recently been carried out.[13-16]

In this work, we calculated dose distributions, produced by proton beam grid irradiations, using real patient composition data. Using proton beams, instead of photons, enables better protection of sensitive risk organs located posterior to the target due to their limited range in tissue. The aim of this work was to study whether it is possible to produce a dose distribution with a well-defined grid structure throughout the normal radiation-sensitive tissue while delivering a more uniform dose (with a high minimum dose) to a large, deep-seated target, containing solid cancer growth. For this purpose, we explored the use of cross-firing of proton beam grids over the target volume. Cross-firing allows for a larger separation between the beam elements incident from each direction than what would have been possible if only 1 beam grid would have been used to irradiate the whole target volume with a uniform dose. That, in turn, makes it possible to maintain a low dose in between the beam elements of the grid, which has been shown to be of importance to keep the toxicity at a low level for the grid therapy carried out in the past. Even though the dose–volume effect has only been systematically studied for a few organs and biological endpoints, we hypothesize that many of the organs traversed by the beam array exhibit an increased radiation tolerance if irradiated with grids containing small beams (width <1.5 cm) instead of with conventional beams, used clinically, of widths of several centimeters.[4]

Modern proton therapy centers provide the possibility to perform so-called spot scanning, which makes it possible to scan the proton pencil beam in a grid-like pattern without added collimation. The divergence of the scanned proton beam is small. Therefore, the elemental beams, building up the grid, will be quasi-parallel and nonoverlapping. However, Coulomb scattering will widen the elemental proton beams with increasing depth in tissue.

We regard this study as a first step in the development of a new grid therapy method. We expect the target dose to be more inhomogeneous than what is typically created when cross-firing uniform beams. Therefore, we suggest that proton grid therapy (PGT) with cross-firing could be used for treating solid tumor growth. If the minimum dose is high enough, the therapeutic objectives could be reached, despite a more fluctuating target dose. At the moment, we are mainly focused on the dosimetric possibilities offered by such a technique. The dose prescription that should be used for this type of treatment and whether the suggested technique should be combined with other therapies are not dealt with in this study. Issues regarding organ motion, setup and range uncertainties, and the validity of radiobiological assumptions are only briefly discussed here and will be addressed separately in more detail at later stages of this project. The patient computed tomography (CT) data sets with delineated structures used in this study (from 1 patient with liver cancer and 1 patient with rectal cancer) have been selected based on the shape, size, and location within the body of the planning target volumes (PTVs). Whether these 2 specific cancer types are suitable to treat with PGT must be determined based on several other medical considerations than what is considered in this work.

Methods and Materials

Irradiation Setup

Two types of proton beam grids were evaluated in this work:

- A 1-dimensional (1-D) grid with narrow rectangular (“planar”) beams (Figure 1A)
- A 2-dimensional (2-D) grid with circular beam elements (Figure 1B)

The total beam area in each array is different for these 2 cases. With the intention of producing a more homogeneous dose to the target volume, an approach with an interlaced cross-firing irradiation technique was attempted (Figure 2). This method has been developed in the microbeam grid radiotherapy research but it has not yet been used clinically.[17-19] With this technique, the target is irradiated with grids of beams incident from different directions. By slightly shifting the grid position in a direction perpendicular to the direction of the beam grid propagation, the beam grids can be interlaced at a certain depth.

For each proton beam grid plan created, 4 different irradiation setups were evaluated: 2 opposing 1-D grids, 2 opposing 2-D grids, 2 × 2 opposing 1-D grids, and 2 × 2 opposing 2-D grids. The last 2 of these setups are shown in Figure 2.

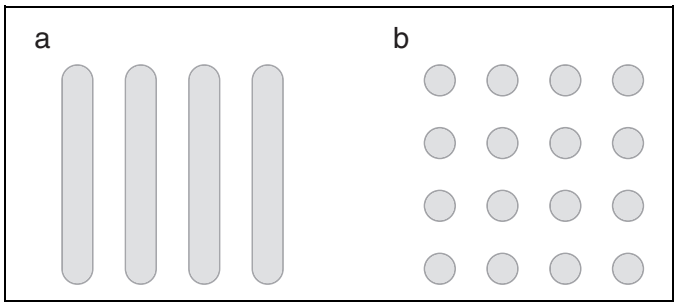

Figure 1. A, One-dimensional (1-D) beam grid containing rectangular-shaped beam elements. B, Two-dimensional (2-D) beam grid containing circular-shaped beams.

Patient Data and Treatment Planning

With prior permission, CT data with delineated structures from 2 anonymous Karolinska Hospital patients, previously treated with conventional photon radiotherapy for either liver or rectal cancer, were used for this study.

All of the grid plans were prepared using the Varian Eclipse treatment planning system version 13 (Varian Medical Systems, Palo Alto, California). The proton beam data from the Skandion proton therapy center, with available energies from 70 to 235 MeV, were employed. The smallest available beam size (full width at half maximum, FWHM) at the patient skin currently available at the Skandion clinic was used for the elemental beams in the grid. It is varying in the range from 7 to 10 mm, depending on the incident proton energy. A spot spacing of 8 mm was chosen to build the grid pattern since it was of similar size as the beam FWHM, which was considered suitable for the interlaced cross-firing.

For the maximum proton kinetic energy considered in this work (235 MeV), the maximum kinetic energy of secondary electrons will be $\sim$0.5 MeV. The maximum range in tissue for this electron energy is less than 2 mm, which means that the electrons produced near the beam edge will not reach midway between the 2 neighboring elemental beams in the grid. However, the incident proton beams have a Gaussian spatial distribution, which means that a small fraction of the protons will be incident on the patient also in between the beam elements and produce dose there.

The treatment fields (the proton beam grids) were created in a stepwise process. Multifield optimization, that is, intensity-modulated proton therapy (IMPT), of regular broad proton beams was first of all performed with a homogeneous dose objective set for the PTV. One hundred percent of the PTV should receive 100% of the prescribed dose (priority = 100). To prevent too large dose inhomogeneities inside the PTV, an additional restriction was included. Only 5% of the target volume was allowed to receive more than 120% of the prescribed dose (priority = 50). This first optimization resulted in 2 or 4 (depending on the number of grids used) rather uniform fields, without any grid pattern. In the next step, the ''edit spots'' built-in functionality of Eclipse was used to delete selected spots and thereby build the grid pattern. For the 1-D grid irradiations, every second vertical line of spots was deleted, whereas for the 2-D grid irradiations, every second vertical and horizontal line of spots were deleted. After performing the spot deletions, the center-to-center distance between 2 beam elements inside a grid was 16 mm. To produce the interlacing, the spots that were deleted in 1 field were kept in the opposing field and vice versa. Finally, using the same objectives and priorities as used initially, but with the new spot maps, a second optimization was performed. The dose distributions were normalized to 100% at the point of PTV minimum dose. A few initial calculation tests showed that if the spot spacing was set to a larger value than the 8 mm chosen, for example, 10 mm (ie, 20 mm after the spot deletion), it was not possible for the optimization algorithm to reach the optimization objectives.

The dose-volume histograms (DVHs) for the PTVs were then extracted and compared for the different grid plans prepared. Furthermore, the conformity index (CI), defined as the ratio between the volume receiving 100% of the prescribed dose and the PTV volume, was determined. Intensity-modulated proton therapy has been shown to be sensitive to organ motion and setup errors.[20] We also evaluated the robustness of the treatment against setup errors by varying the position or the rotation angle of one of the incident beam arrays.

Results

In Figure 3A and B, coronal views of the patient with rectal cancer are shown at a tissue depth of 7 cm (3 cm upstream from the target) with superimposed dose distributions produced by a 1-D grid or a 2-D grid irradiation, respectively. As shown in these figures, the dose distributions produced by the individual beam elements were well separated at this depth. The small divergence of the proton beams and the short range of the secondary electrons produced created a low dose in between the beam elements down to depths, where the Coulomb scattering had widened the proton beams considerably.

In Figure 4A to D, it can be observed that it was possible to maintain a grid-shaped dose pattern from the skin down to the proximity of the PTV, even though the beams are densely spaced. Despite the preserved grid pattern of the delivered dose close to the target surface, satisfying dose coverage of the target was achieved by combining the interlacing and cross-firing techniques. The choice of beam setup (1-D or 2-D grids and the number of grids used) has an important impact on the produced dose distributions. For the case depicted in Figure 4A, for which only 2 opposing 1-D grids were used, the target dose was rather homogeneous, ranging from 100% to 116%, with a mean dose of 111%. The maximum peak dose in the elemental beams outside the target was approximately 71% at a distance of 2 cm from the target. As shown in Figure 4B, a higher level of homogeneity could be produced inside the target when using 2 $\times$ 2 opposing 1-D grids (mean dose = 107%; maximum dose = 113%). The maximum peak dose outside the PTV also decreased to 46%. Similar results were obtained for the rectal cancer case with this geometry (Figure

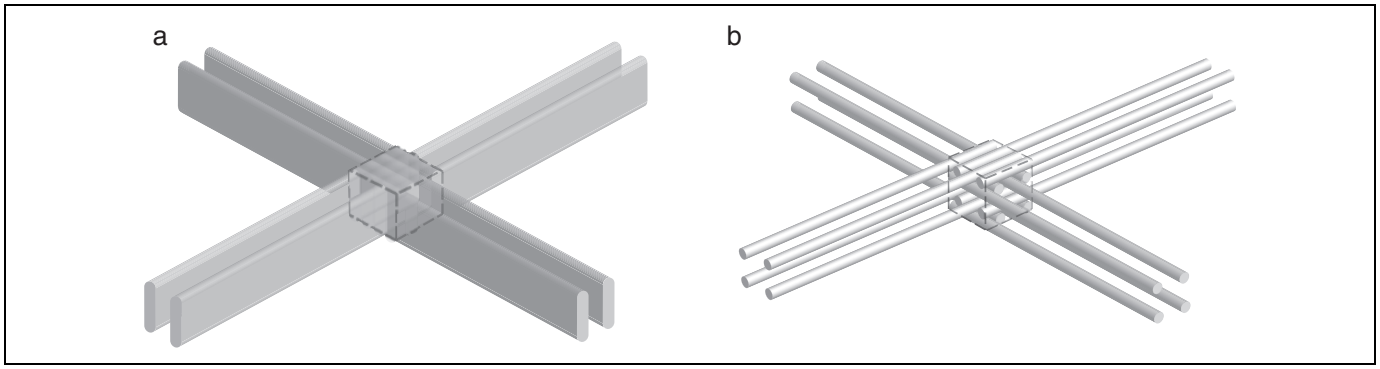

Figure 2. Interlacing of 4 beam grids inside a hypothetical cubic target volume (dashed box). A, One-dimensional (1-D) beam grids. B, Two-dimensional (2-D) beam grids.

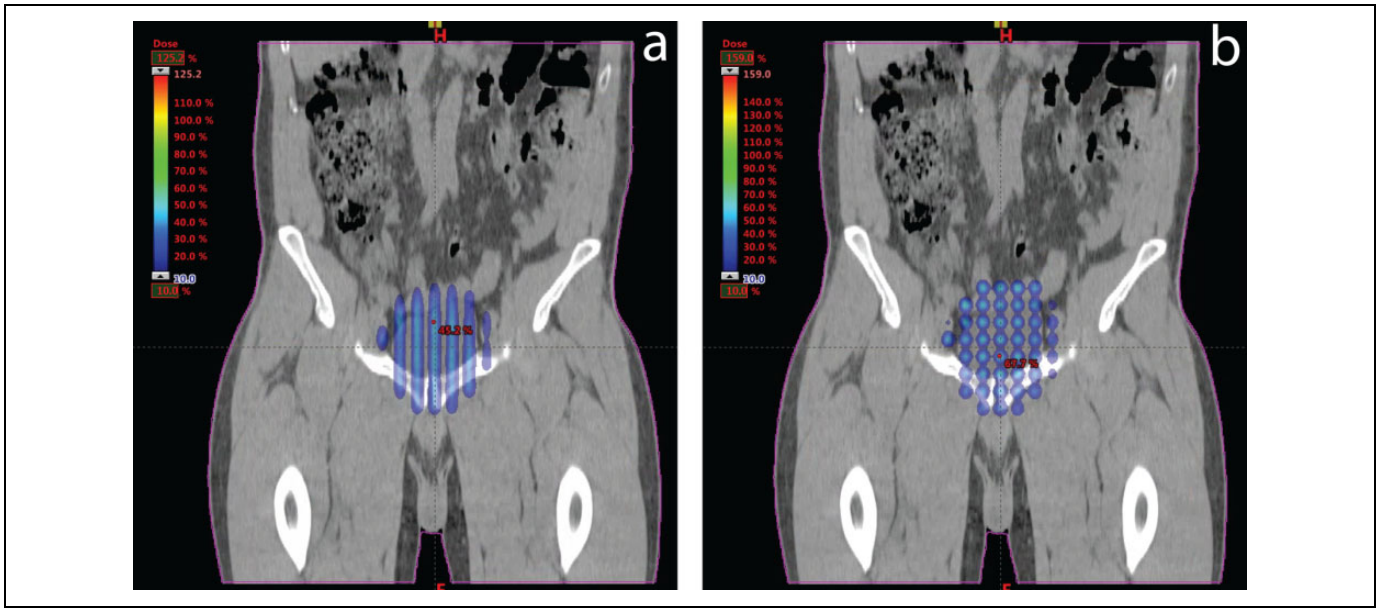

Figure 3. Dose distributions obtained for the 2 types of grid irradiations considered in this work superimposed on coronal computed tomography (CT) sections from the patient with rectal cancer. A, One-dimensional (1-D) grid. B, Two-dimensional (2-D) grid.

4C), with PTV mean and maximum doses of 114% and 125%, respectively. The use of 2 × 2 opposing 2-D grids (Figure 4D) created a mean dose of 120% and a maximum dose of 142% inside the target, but higher doses were also delivered in the beams outside the PTV. This tendency could be noted especially at the skin entrance where the relative maximum dose was approximately 82%. Figure 5 shows the differential PTV-DVHs for the liver and rectal cancer target irradiations for each of the beam setups studied in this work.

The maximum peak and valley doses at the skin entrance and at a position 2 cm anterior (upstream) to the PTV are summarized in Table 1, as well as the mean and maximum doses inside the PTV. Since large fluctuations of the valley and peak doses could be observed for each irradiation setup (even within the same grid), only the maximum valley and peak doses at the different locations were recorded. Of all the cases studied, the 2 × 2 opposing 1-D grid geometry produced the highest dose homogeneity inside the target. On the other hand, the 2 × 2 opposing 2-D grid geometry produced the highest mean and maximum target doses, indicating that it is difficult to avoid cold spots in the target with this setup. Because a smaller total beam area is used with this configuration, the peak doses outside the PTV must be increased in order to deliver a satisfying minimum target dose.

In Figure 6, the variation in the peak and valley doses with depth is shown inside one of the 1-D and one of the 2-D beam grids used for the irradiation of the rectal cancer target, as shown in Figure 4C and D, respectively. The doses produced inside the anterior treatment grids were studied and the dose profiles were recorded at the center of these grids. The peak-to-valley dose ratios (PVDRs) ranged from approximately 9 at the skin to 5, 2 cm anterior to the PTV, inside both of these grids. Finally, the PVDRs were approximately 1 or 1.1 inside the PTV for the 1-D or 2-D beam grids, respectively. The target dose homogeneity was somewhat lower for the 2-D beam grid irradiation setup.

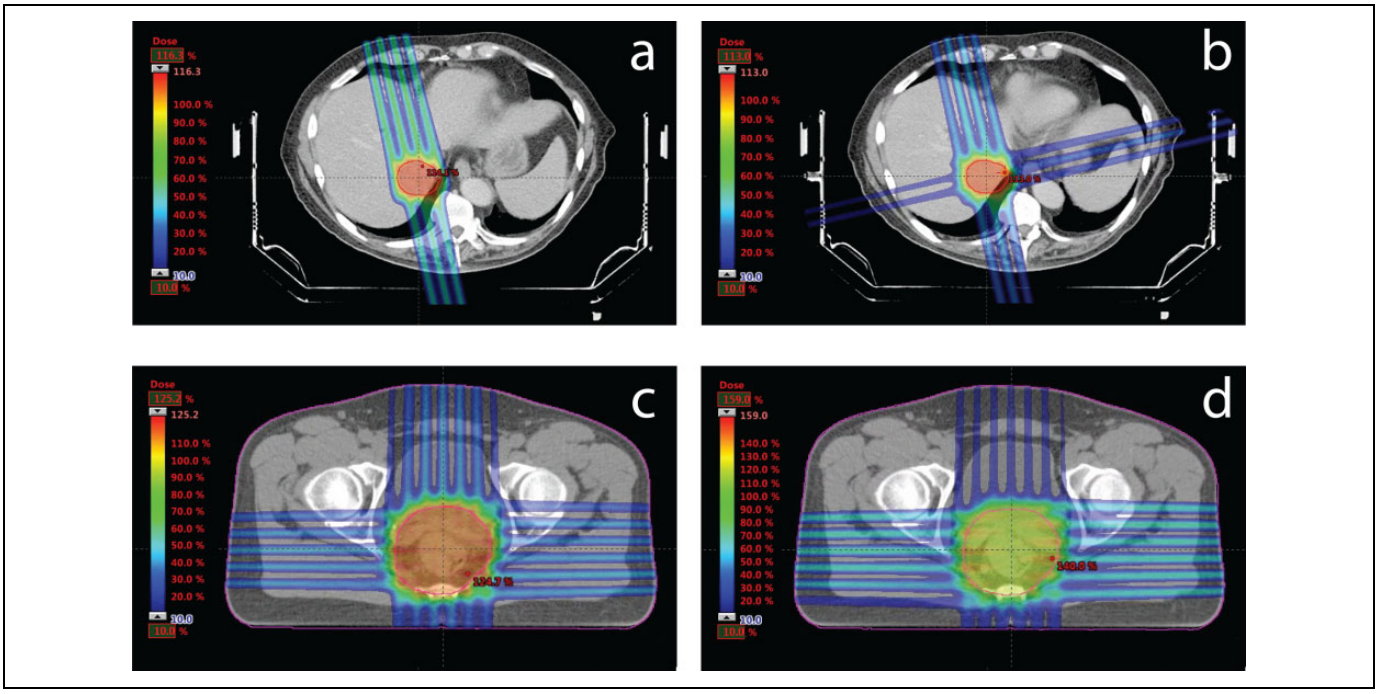

Figure 4. Planned dose distributions obtained for the grid irradiations superimposed on axial computed tomography (CT) sections from the 2 patient cases studied: (A) liver cancer, 2 opposing 1-dimensional (1-D) grids, (B) liver cancer, 2 × 2 opposing 1-D grids (C) rectal cancer, 2 × 2 opposing 1-D grids, and (D) rectal cancer, 2 × 2 opposing 2-dimensional (2-D) grids. CT indicates computed tomography; 1-D, 1-dimensional; 2-D, 2-dimensional.

In Table 2, the doses received by 95% and 50% of the PTV are presented for both the liver and rectal cancer treatments for the 4 different grid irradiation techniques evaluated. The CI is also shown. Higher $D_{95\%}$, $D_{50\%}$, and CI can be observed for the 2-D grid irradiation setups.

A situation in which one of the grids used in the cross-firing was translated or rotated was also studied to determine the robustness of the proposed grid irradiation to realistic setup uncertainties. Gantry angular shifts of 1°, 2°, and 3° were considered as well as lateral translations (perpendicular to the beam propagation) of the patient position of 1 and 2 millimeters. In Table 3, the resulting minimum, maximum, and mean doses inside the target after the translations or shifts of one of the grids are presented. Due to the rather poor target dose uniformity obtained for the irradiation geometry with 2 opposing 2-D grids, it was excluded from this part of the study.

The use of 4 beam grids instead of 2 increased the robustness of the treatment to small setup errors. In most cases, a shift in the gantry angle of 1 grid had only a small effect on the final dose distribution in the target. However, a lateral shift of one of the beam grids caused bigger fluctuations. In that case, the peaks of the shifted grid are getting closer to the peaks of the opposing grid instead of coinciding with the valleys. As a result, hot and cold spots appear. The mean target dose, on the other hand, was unaffected by setup errors as can be expected. In small volumes containing normal tissue, located next to the target, the doses in some cases increased with up to 10% as a result of the setup errors. Since these hot spot volumes are small, we do not expect them to increase the treatment toxicity significantly. Further away from the target (at more than a few mm distance), the size of doses given to the skin and other normal tissues remained unchanged.

Discussion

The results of this work showed that it is possible to create a rather uniform dose (with a high minimum dose) inside the PTV by cross-firing proton beam grids. Similar dose homogeneity can be achieved with PGT as with more conventional treatment techniques, for example, stereotactic body radiation therapy (SBRT).[21] The choice of irradiation geometry, that is, beam grid type and the numbers of grids used, was shown to have an important impact on the dose homogeneity that could be achieved inside the PTV. Cross-firing of beam grids, containing either ion or photon beam elements, over a target volume has previously been suggested.[22-25] In previous studies of proton beam grid therapy, the aim has normally been to create a uniform target dose.[15,16,23] On the contrary, when photon beam grids have been considered for cross-firing, the aim has often been to produce a highly nonuniform target dose, reminiscent of what can be created in brachytherapy.[22,24,25] It is evident that it is possible to create nonuniform target doses also with proton beam grid irradiations. However, existing tumor control probability models indicate that an improved therapeutic effect can be obtained if the minimum target dose is sufficiently elevated.[26] We have shown in this work that a high minimum target dose can be produced with the proposed interlaced cross-firing PGT technique, without irradiating any risk organ

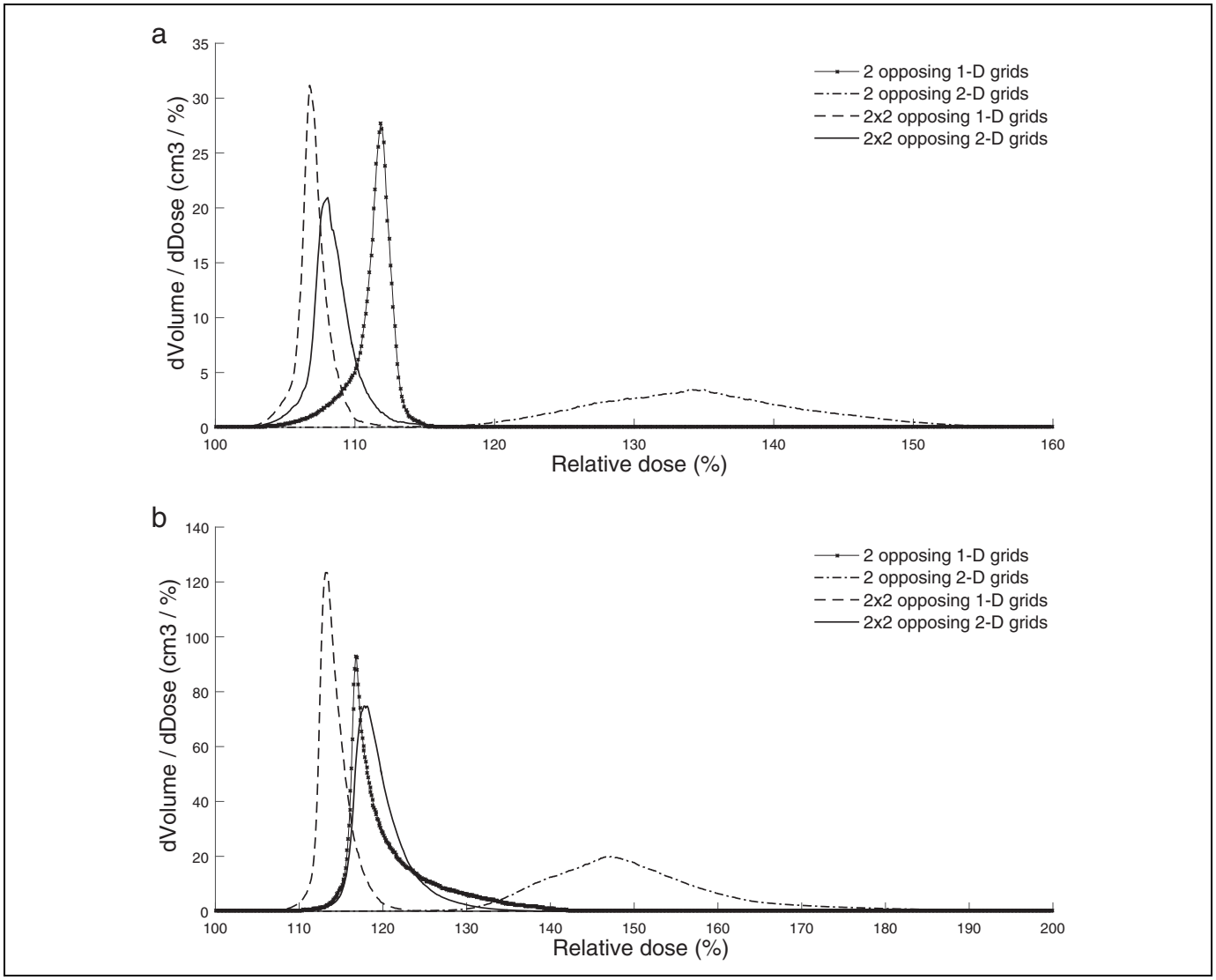

Figure 5. Differential dose-volume histograms (DVHs) for the planning target volumes (PTVs) obtained with the different irradiation setups evaluated in this work for (A) the liver cancer treatment and (B) the rectal cancer treatment.

from more than 1 direction. This will be more difficult to achieve with photon-based grid therapy with divergent beams.

Furthermore, we have demonstrated that it is possible to preserve the grid structure of the dose distribution down to the depth of the target volume if cross-firing is used. This distinguishes this work from previous studies done on proton beam grid therapy,[15,16] in which a homogenous dose has been produced for each incident beam grid. Keeping the grid structure of the dose distribution down to the direct vicinity of the target (with high doses restricted to small volumes) could be of importance to prevent side effects. In photon beam–based radiosurgery, the tissue volume immediately surrounding the target is normally given high doses. It is in these tissue volumes that the risk of radiation-induced side effects after radiosurgery has been shown to be the highest, for example, in the brain.[27] For extracranial SBRT, there is to our knowledge no detailed report describing which metric is the most appropriate for predicting the risk of side effects.

The DVHs for the normal tissue extracted from the grid therapy planning (not shown in this article) give an indication of which dose levels are present in this tissue but cannot be used for a direct estimation of the negative side effects of the treatment. The reason is that the DVHs show a summary of the doses given to independent volumes regardless of whether spatial fractionation is used. The DVHs in that sense depend only on the total beam area used to irradiate a delineated volume.

In this work, we have investigated the possibility to perform proton grid treatments with beam sizes and energies available at modern proton facilities using a commercial treatment planning system. However, substantial evidence from preclinical research indicates that the use of even smaller beams could improve the normal tissue tolerance to this type of treatment even further.[12,13,18] Further studies to determine suitable proton beam collimation techniques are required to develop a therapeutic method using beam widths of only 1 or a few millimeters. Moreover, the increase in the tolerance doses with

Table 1. Summary of Data for Selected Dosimetric Variables Obtained From the Created Treatment Plans.[a]

		Skin Dose		Dose 2 cm Before PTV		Dose Inside PTV	
Treatment Case	Irradiation Technique	Max Valley (%)	Max Peak (%)	Max Valley (%)	Max Peak (%)	Max (%)	Mean (%)
Liver	2 opposing 1-D grids	10	69	21	71	116	111
	2 opposing 2-D grids	20	138	35	125	169	135
	2 × 2 opposing 1-D grids	4	46	15	51	113	107
	2 × 2 opposing 2-D grids	6	120	25	67	119	108
Rectum	2 opposing 1-D grids	6	92	18	84	147	119
	2 opposing 2-D grids	15	202	35	159	216	152
	2 × 2 opposing 1-D grids	5	58	10	56	125	114
	2 × 2 opposing 2-D grids	6	82	12	64	142	120

Abbreviations: 1-D, 1-dimensional; 2-D, 2-dimensional; Max, maximum; PTV, planning target volume.
[a] The normalization (100%) was done to the minimum target dose.

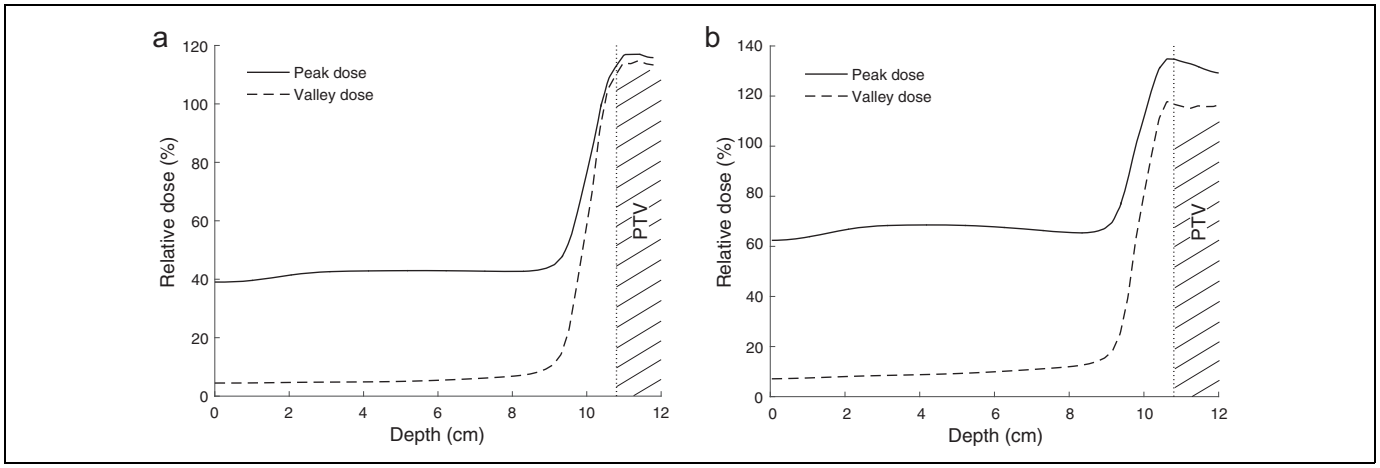

Figure 6. The variation in the peak and valley doses with depth is shown inside the beam grids, incident anteriorly on the patient with rectal cancer. A, One-dimensional (1-D) grid. B, Two-dimensional (2-D) grid.

Table 2. Representative Dosimetric Characteristics of the PTV Coverage for the Different Grid Irradiation Setups Evaluated.

Structure	Irradiation Technique	Volume (cm^3)	$D_{95\%}$ (%)	$D_{50\%}$ (%)	CI
PTV_{Liver}	2 opposing 1-D grids	59.6	108	111	1.36
	2 opposing 2-D grids		123	134	2.05
	2 × 2 opposing 1-D grids		105	107	1.22
	2 × 2 opposing 2-D grids		106	108	1.29
PTV_{Rectum}	2 opposing 1-D grids	409.2	115	118	1.39
	2 opposing 2-D grids		134	151	1.75
	2 × 2 opposing 1-D grids		112	114	1.24
	2 × 2 opposing 2-D grids		116	119	1.32

Abbreviations: CI, conformity index; 1-D, 1-dimensional; 2-D, 2-dimensional; PTV, planning target volume.

decreasing beam sizes for different organs and endpoints must be more accurately determined to establish a clinical advantage of PGT. The prescription doses that should be administered and whether fractionation should be used must also be decided. The possibility to use this treatment as a boost will be evaluated further on.

In this work, the IMPT method was used to produce the treatment plans for the grid irradiations. The proton range uncertainties are important to consider in IMPT when the proton beam path goes through tissue with a density that varies with, for example, the breathing motion. Intensity-modulated proton therapy has previously been suggested for the treatment of abdominal cancer by other authors.[28,29] We expect that the range uncertainties will have a similar impact on the delivered doses in PGT as for other types of proton beam treatments. The range uncertainties are affecting the dose distribution along the beam grid propagation direction. These will therefore not deteriorate the beam grid characteristics. We suggest irradiations

Table 3. The Variation in the Target Dose Due to Simulated Gantry Angle or Patient (Table) Position Setup Errors for One of the Grids Used in the Irradiation.[a]

Target	Irradiation Technique	Shift	Relative Dose (%)		
			Min	Max	Mean
Liver cancer	2 opposing 1-D grids	0° | 1° | 2° | 3°	100.0 | 97.9 | 95.7 | 93.2	116.0 | 116.4 | 118.3 | 121.1	111.2 | 111.2 | 111.1 | 111.0
		0 mm | 1 mm | 2 mm	100.0 | 93.2 | 85.9	116.0 | 124.7 | 132.8	111.2 | 111.2 | 111.3
	2 × 2 opposing 1-D grids	0° | 1° | 2° | 3°	100.0 | 100.1 | 99.0 | 97.2	113.2 | 113.2 | 113.2 | 114.6	107.0 | 107.0 | 107.0 | 106.8
		0 mm | 1 mm | 2 mm	100.0 | 95.6 | 90.4	113.2 | 118.4 | 124.2	107.0 | 107.0 | 107.1
	2 × 2 opposing 2-D grids	0° | 1° | 2° | 3°	100.0 | 99.8 | 99.5 | 99.2	119.0| 118.7 | 118.5 | 117.9	108.4 | 108.4 | 108.4 | 108.4
		0 mm | 1 mm | 2 mm	100.0 | 95.6 | 91.6	119.0 | 119.7 | 122.8	108.4 | 108.6 | 108.7
Rectal cancer	2 opposing 1-D grids	0° | 1° | 2° | 3°	100.0 | 95.4 | 88.8 | 82.2	146.7 | 146.9 | 147.6 | 148.6	118.5 | 118.5 | 118.5 | 118.5
		0 mm | 1 mm | 2 mm	100.0 | 95.2 | 84.6	146.7 | 147.3 | 155.0	118.5 | 118.5 | 118.3
	2 × 2 opposing 1-D grids	0° | 1° | 2° | 3°	100.0 | 97.3 | 94.4 | 90.5	124.5 | 124.8 | 126.4 | 130.5	114.2 | 114.2 | 114.2 | 114.2
		0 mm | 1 mm | 2 mm	100.0 | 98.7 | 92.4	124.5 | 128.8 | 133.7	114.2 | 114.2 | 114.1
	2 × 2 opposing 2-D grids	0° | 1° | 2° | 3°	100.0 | 100.0 | 99.5 | 98.0	142.0 | 141.3 | 141.2 | 142.4	119.7 | 119.7 | 119.7 | 119.8
		0 mm | 1 mm | 2 mm	100.0 | 98.1 | 96.1	142.0 | 142.2 | 145.7	119.7 | 119.7 | 119.7

Abbreviations: 1-D, 1-dimensional; 2-D, 2-dimensional; Min, minimum; Max, maximum.
[a] The normalization (100%) was done to the minimum target dose for the case without setup errors.

from several angles (as was done in this work) to improve the target dose coverage, the treatment robustness, and to reduce the peak doses given to normal tissue. Furthermore, since we aim to irradiate solid tumors, minor fluctuations in the target dose will be less important as compared to the situations when smaller targets with microscopic spread are treated, as long as the minimum dose is sufficiently high. If the cross-fired proton beam grids are misaligned, due to, for example, organ motion, the target dose will become more inhomogeneous and more similar to what is typically achieved with photon beam–based grid therapy. Methods such as image-guided radiotherapy, abdominal pressure, gating, and rescanning can of course also be used to further reduce the treatment delivery uncertainties.

Conclusion

The PGT method suggested in this work can be offered by proton therapy centers equipped with spot scanning capabilities. With PGT, a rather homogeneous and high dose can be produced in a deep-seated target, while the grid structure of the dose distribution can be maintained down to the vicinity of the target volume (with a low dose in between the beams). By cross-firing 1-D proton beam grids, a more uniform target dose, with a CI closer to 1.0, can be produced than with 2-D proton beam grids. We anticipate that the high minimum dose given to the target by cross-firing the proton beam grids will translate into an increased tumor control probability, compared to what can be obtained with the highly nonhomogenous target dose obtained with unidirectional photon beam grid irradiations. We also expect that a high degree of normal tissue sparing can be obtained because the normal tissue is only irradiated with grids of small beams down to large depths. A sensitivity test showed that treatments with 4 interlaced proton beam grids are reasonably robust against setup errors.

Declaration of Conflicting Interests

The author(s) declared no potential conflicts of interest with respect to the research, authorship, and/or publication of this article.

Funding

The author(s) disclosed receipt of the following financial support for the research, authorship, and/or publication of this article: Financial support from the Cancer Research Funds of Radiumhemmet is gratefully acknowledged.

References

1. Laissue JA, Blattmann H, Slatkin DN. Alban Köhler (1874-1947): inventor of grid therapy [in German]. *Z Med Phys*. 2012;22(2): 90-99. doi:10.1016/j.zemedi.2011.07.002.
2. Laissue JA, Blattmann H, Slatkin DN. CORRIGENDUM to "Alban Köhler (1874-1947): Erfinder der Gittertherapie". *Z Med Phys.* 22 (2012) 90-99. *Z Med Phys*. 2013;23(4). doi:10.1016/j.zemedi.2013.09.007.
3. Köhler A. Une nouvelle méthode permettant de faire agir, dans la profondeur des tissus, de hautes doses de rayons Roentgen et un

moyen nouveau de protection contre les radiodermites. *Ann d'Electrobiologie Radiol*. 1909;10:661-664.
4. Haring W. Siebstrahlung. *Strahlentherapie*. 1934;51:154-163.
5. Mohiuddin M, Fujita M, Regine WF, Megooni AS, Ibbott GS, Ahmed MM. High-dose spatially-fractionated radiation (GRID): a new paradigm in the management of advanced cancers. *Int J Radiat Oncol Biol Phys*. 1999;45(3):721-727.
6. Neuner G, Mohiuddin MM, Vander Walde N, et al. High-dose spatially fractionated GRID radiation therapy (SFGRT): a comparison of treatment outcomes with Cerrobend vs. MLC SFGRT. *Int J Radiat Oncol Biol Phys*. 2012;82(5):1642-1649. doi:10.1016/j.ijrobp.2011.01.065.
7. Peñagarícano JA, Moros EG, Ratanatharathorn V, Yan Y, Corry P. Evaluation of spatially fractionated radiotherapy (GRID) and definitive chemoradiotherapy with curative intent for locally advanced squamous cell carcinoma of the head and neck: initial response rates and toxicity. *Int J Radiat Oncol Biol Phys*. 2010;76(5):1369-1375. doi:10.1016/j.ijrobp.2009.03.030.
8. Mohiuddin M, Curtis DL, Grizos WT, Komarnicky L. Palliative treatment of advanced cancer using multiple nonconfluent pencil beam radiation. A pilot study. *Cancer*. 1990;66(1):114-118.
9. Mohiuddin M, Park H, Hallmeyer S, Richards J. High-dose radiation as a dramatic, immunological primer in locally advanced melanoma. *Cureus*. 2015;7(12):e417. doi:10.7759/cureus.417.
10. Kaiser A, Mohiuddin MM, Jackson GL. Dramatic response from neoadjuvant, spatially fractionated GRID radiotherapy (SFGRT) for large, high-grade extremity sarcoma. *J Radiat Oncol*. 2013;2(1):103-106. doi:10.1007/s13566-012-0064-5.
11. Hopewell JW, Trott KR. Volume effects in radiobiology as applied to radiotherapy. *Radiother Oncol*. 2000;56(3):283-288.
12. Bijl HP, van Luijk P, Coppes RP, Schippers JM, Konings AWT, van der Kogel AJ. Dose-volume effects in the rat cervical spinal cord after proton irradiation. *Int J Radiat Oncol Biol Phys*. 2002;52(1):205-211.
13. Bräuer-Krisch E, Serduc R, Siegbahn EA, et al. Effects of pulsed, spatially fractionated, microscopic synchrotron X-ray beams on normal and tumoral brain tissue. *Mutat Res*. 2010;704(1-3):160-166. doi:10.1016/j.mrrev.2009.12.003.
14. Laissue JA, Bartzsch S, Blattmann H, et al. Response of the rat spinal cord to X-ray microbeams. *Radiother Oncol*. 2013;106(1):106-111. doi:10.1016/j.radonc.2012.12.007.
15. Dilmanian FA, Eley JG, Krishnan S. Minibeam therapy with protons and light ions: physical feasibility and potential to reduce radiation side effects and to facilitate hypofractionation. *Int J Radiat Oncol Biol Phys*. 2015;92(2):469-474. doi:10.1016/j.ijrobp.2015.01.018.
16. Zlobinskaya O, Girst S, Greubel C, et al. Reduced side effects by proton microchannel radiotherapy: study in a human skin model. *Radiat Environ Biophys*. 2013;52(1):123-133. doi:10.1007/s00411-012-0450-9.
17. Bräuer-Krisch E, Requardt H, Régnard P, et al. New irradiation geometry for microbeam radiation therapy. *Phys Med Biol*. 2005;50(13):3103-3111. doi:10.1088/0031-9155/50/13/009.
18. Dilmanian FA, Zhong Z, Bacarian T, et al. Interlaced x-ray microplanar beams: a radiosurgery approach with clinical potential. *Proc Natl Acad Sci U S A*. 2006;103(25):9709-9714. doi:10.1073/pnas.0603567103.
19. Serduc R, Bräuer-Krisch E, Siegbahn EA, et al. High-precision radiosurgical dose delivery by interlaced microbeam arrays of high-flux low-energy synchrotron X-rays. *PLoS One*. 2010;5(2):e9028. doi:10.1371/journal.pone.0009028.
20. Lomax AJ. Intensity modulated proton therapy and its sensitivity to treatment uncertainties 2: the potential effects of inter-fraction and inter-field motions. *Phys Med Biol*. 2008;53(4):1043-1056. doi:10.1088/0031-9155/53/4/015.
21. Lax I, Blomgren H, Näslund I, Svanström R. Stereotactic radiotherapy of malignancies in the abdomen. Methodological aspects. *Acta Oncol*. 1994;33(6):677-683.
22. Meigooni AS, Gnaster M, Dou K, Johnson EL, Meigooni NJ, Kudrimoti M. Dosimetric evaluation of parallel opposed spatially fractionated radiation therapy of deep-seated bulky tumors. *Med Phys*. 2007;34(2):599-603. doi:10.1118/1.2431423.
23. Lomax AJ, Schaer M. 322 intensity modulated "grid" proton therapy. Trying to exploit "spatial fractionation" with protons. *Radiother Oncol*. 2012;102(Suppl 1):S171-S173. doi:10.1016/S0167-8140(12)70282-7.
24. Jin JY, Zhao B, Kaminski JM, et al. A MLC-based inversely optimized 3D spatially fractionated grid radiotherapy technique. *Radiother Oncol*. 2015;117(3):483-486. doi:10.1016/j.radonc.2015.07.047.
25. Zhang X, Penagaricano J, Yan Y, et al. Spatially fractionated radiotherapy (GRID) using helical tomotherapy. *J Appl Clin Med Phys*. 2016;17(1):5934.
26. Brahme A. Dosimetric precision requirements in radiation therapy. *Acta Radiol Oncol*. 1984;23(5):379-391.
27. Flickinger JC, Kano H, Niranjan A, Kondziolka D, Lunsford LD. Dose selection in stereotactic radiosurgery. *Prog Neurol Surg*. 2013;27:49-57. doi:10.1159/000341623.
28. Petersen JBB, Lassen Y, Hansen AT, Muren LP, Grau C, Høyer M. Normal liver tissue sparing by intensity-modulated proton stereotactic body radiotherapy for solitary liver tumours. *Acta Oncol*. 2011;50(6):823-828. doi:10.3109/0284186X.2011.590526.
29. Radu C, Norrlid O, Brændengen M, Hansson K, Isacsson U, Glimelius B. Integrated peripheral boost in preoperative radiotherapy for the locally most advanced non-resectable rectal cancer patients. *Acta Oncol*. 2013;52(3):528-537. doi:10.3109/0284186X.2012.737022.